Journal of Alloys and Compounds 745 (2018) 228–233

Contents lists available at ScienceDirect

Journal of Alloys and Compounds

journal homepage: http://www.elsevier.com/locate/jalcom

Increasing the thermoelectric power factor via Ag substitution at Zn site in $Ba(Zn_{1-x}Ag_x)_2Sb_2$

Ruijuan Yan [a, 1], Jianwei Lin [a], Li You [a], Kai Guo [a, *], Xinxin Yang [a, **], Jiye Zhang [a], Dongli Hu [a], Jun Luo [a], Jing-Tai Zhao [a, b]

[a] School of Materials Science and Engineering, Shanghai University, Shanghai 200444, China
[b] State Key Laboratory of Advanced Special Steel, Shanghai University, Shanghai 200444, China

ARTICLE INFO

Article history:
Received 20 November 2017
Received in revised form
6 February 2018
Accepted 12 February 2018
Available online 15 February 2018

Keywords:
$BaZn_2Sb_2$
Zintl phase
Carrier concentration
Thermoelectric materials

ABSTRACT

Antimony-based Zintl compounds AZn_2Sb_2 (A = Ca, Sr, Ba, Eu, Yb) have been considered as an appealing thermoelectric system for developing the Zintl structure-property relationship and exploring novel thermoelectric materials. Differing from trigonal layered phases as represented by $EuZn_2Sb_2$, $BaZn_2Sb_2$ adopts a channel structure (*Pnma*) constructed by anionic framework $[Zn_2Sb_2]^{2-}$ and cationic Ba^{2+}. Polycrystalline bulk samples of $Ba(Zn_{1-x}Ag_x)_2Sb_2$ ($0 \le x \le 0.01$) were prepared by a solid-state reaction method and subsequent hot press sintering aiming at higher thermoelectric figure of merit. Seebeck coefficient, electrical and thermal conductivities of all the samples were measured in the temperature range 323–760 K. The substitution of Zn by Ag effectively improves the electrical transport properties through optimization of hole concentration. Of all the samples, $Ba(Zn_{0.996}Ag_{0.004})_2Sb_2$ shows the highest thermoelectric power factor (9.45 μW cm^{-1} K^{-2}@567 K) and figure of merit ZT (0.63@760 K), permitting the substitution strategy in anionic framework of Zintl phase for increasing thermoelectric efficiency.

1. Introduction

Thermoelectric (TE) materials, which can realize the direct interconversion of electricity and heat powers, have been utilized for waste heat recovery, powering in the deep space exploring and cooling sensitive electronics for decades [1–4]. To broaden the practical application, the thermoelectric properties of TE materials are required to be improved in order to achieve sufficient conversion efficiency of heat into electricity. In principle, the thermoelectric performance of TE materials is determined by the dimensionless figure of merit $ZT = S^2\sigma T/(\kappa_E + \kappa_L)$, where S (μV K^{-1}) is the Seebeck coefficient, σ (S m^{-1}) is the electrical conductivity, κ_E is the electronic component and κ_L is the lattice component of thermal conductivity ($\kappa = \kappa_E + \kappa_L$, W m^{-1} K^{-1}), and T (K) is the absolute temperature [5,6]. As expected, promising TE materials should possess a combination of excellent electrical conductivity σ, large thermopower S (absolute value) and lower thermal conductivity κ.

For metal or degenerate semiconductors, the electrical conductivity (σ) is related to the carrier concentration n through the carrier mobility μ: $\sigma = ne\mu$, while the Seebeck coefficient is given by: $S = C(\pi/3n)^{2/3}m^*T$, $C = 8\pi^2k_B^2/3eh$ [2]. Here, m^*, e, k_B, h represent the carrier effective mass, electron charge, Boltzmann constant and Plank constant, respectively. Additionally, the electronic thermal conductivity κ_E depending on carrier concentration n can be expressed as: $\kappa_E = L\sigma T = Lne\mu T$ (L is the Lorenz number). The strongly coupled parameters of σ, S and κ_E through n make the enhancement of thermoelectric figure of merit ZT a challenging task [7,8]. An achievable strategy for developing potential thermoelectric systems is optimization of carrier concentration in narrow-band-gap compounds with complex structures probably exhibiting low lattice thermal conductivity [9,10]. The peak of ZT typically occurs at carrier concentrations between 10^{19} and 10^{21} carriers per cm^3, corresponding to heavily doped semiconductors [11,12].

The way has been successfully applied in some Zintl phase compounds, such as clathrates [13], Zn_4Sb_3 [14,15] and $Yb_{14}MnSb_{11}$ [10,16], which feature semiconductor behavior with characteristic structure. Precisely designed doping level and controlled Fermi level can realize the improvement of the electrical transport

* Corresponding author.
** Corresponding author.
E-mail addresses: kai.guo@shu.edu.cn (K. Guo), yangxinxin@shu.edu.cn (X. Yang).
[1] Present address: School of Materials Science and Engineering, Xi'an Jiaotong University, Shaanxi 710049, China.

https://doi.org/10.1016/j.jallcom.2018.02.155
0925-8388/

properties and enable to obtain promising power factor ($PF = S^2\sigma$). In addition, a few simple ternary Zintl phase compounds containing alkali-earth or rare-earth elements such as $Ba_4In_8Sb_{16}$ [17], $Eu_5In_2Sb_6$ [18], $EuCd_2Sb_2$ [19,20], and $BaCu_2Te_2$ [21] have been synthesized and studied as well. $BaZn_2Sb_2$ is isostructural to $BaCu_2Te_2$, adopting an orthorhombic crystal structure where Zn and Sb atoms build up a three-dimensional network using covalent bonds as electrons transport media while Ba atoms are embedded into the empty space as "rattle" heavy atoms contributing low thermal conductivity. Wang et al. firstly investigated the thermoelectric performance of pristine $BaZn_2Sb_2$ and revealed the considerably low thermal conductivity (~1.6 W m^{-1} K^{-1} at 300 K) [22]. Eventually, the *ZT* value reached 0.31 at 675 K without further optimization. Recently, our group reported that substituting Ba by Na and Sr enhanced the power factor and decreased the thermal conductivity simultaneously, increasing the *ZT* value upon 0.58 at 704 K [23]. In this work, the effects of Ag monodoping in the anionic framework of $BaZn_2Sb_2$ on the electrical and thermal transport properties were systematically studied. Ag is introduced at Zn site as acceptor dopant to directly increase the hole concentration, leading to the significant improvement of the thermoelectric properties of $BaZn_2Sb_2$.

2. Experimental section

Ba pieces (99.8%), Zn pellets (99.999%), Ag wires (99.99%) and Sb pieces (99.999%) were used as the starting materials. All manipulations were performed in an argon-filled glove box with the total O_2 and H_2O level below 0.1 ppm. The mixture of all elements of Ba, Zn, Ag and Sb were weighted according to the stoichiometric ratio and placed into alumina crucibles. These assembles were subsequently enclosed in evacuated fused quartz tubes, and annealed in a programmable furnace. The furnace was heated to 1123 K at the rate of 1 K/min, held at this temperature for 3 days, and subsequently cooled to room temperature by switching off the furnace. The obtained bulks were ground into powder and densified by a vacuum hot-press furnace at 913 K for 30 min under a pressure of 50 MPa using a graphite mold. The resulting densities of all samples were about 95% of the theoretical density.

The as-obtained samples were structurally characterized by powder X-ray diffraction (PXRD) on a diffractometer (3 KW D/max2200V, Japan) with Cu Kα ($\lambda = 1.54178$ Å, 60 KV/80 mA) radiation. The microstructures of the polycrystalline $BaZn_2Sb_2$-based samples were examined by scanning electron microscopy (GeminiSEM 300), equipped with electron energy dispersive X-ray spectroscopy (EDS, Oxford X-MAX). The thermal diffusivity coefficient (D) was measured in a pellet-shaped sample with diameter of Φ10 mm and thickness of 1–2 mm by using the laser flash diffusivity (NETZSCH LFA457, Germany). Prior to measurements, the samples were coated with a thin graphite layer to minimize errors from the emissivity of materials. The thermal conductivity of the pellets can be derived from the relationship $\kappa = dC_pD$, where d is the experimental density, C_p is the heat capacity, and D is the experimental thermal diffusivity. The density (d) was measured by automatic density analyzer (Quantachrome ULTRAPYC 1200e, USA) at room temperature. Specific heat capacity (C_p) was derived from the temperature-dependent heat data by comparing with that of sapphire standard sample recorded from the differential thermal analyzer (NETZSCH, STA449F3 Germany). The pellet-shaped samples were cut into small parallelepiped ($3 \times 3 \times 8$ mm^3) for the Seebeck coefficient and electrical conductivity measurement using an Ulvac Riko ZEM-3 instrument (ZEM-3, ULVAC-RIKO, Japan) under a low-pressure helium atmosphere from room temperature to 760 K. The carrier concentration at room temperature were acquired from Hall measurements using the Van der Pauw method on Lakeshore 8404.

3. Results and discussion

The powder X-ray diffraction (PXRD) patterns of as-synthesized polycrystalline $Ba(Zn_{1-x}Ag_x)_2Sb_2$ ($x = 0$, 0.002, 0.004, 0.006, 0.008, 0.01) samples are shown in Fig. 1(a). The simulated pattern of the reported $BaZn_2Sb_2$ (JCPDS card, No.33-0095) [24] is also provided for comparison. Obviously, the main diffraction patterns of these polycrystalline samples can be indexed as an orthorhombic $BaCu_2Te_2$-type structure with space group *Pnma*. Several additional weak peaks from traces of impurity phases such as BaO and ZnSb (marked in Fig. 1(a)) are observed, which maybe resulted from oxygen impurity in reactants. Fig. 1(b) displays the hole concentration in bulk samples $Ba(Zn_{1-x}Ag_x)_2Sb_2$ ($x = 0$, 0.002, 0.004, 0.006, 0.008, 0.01) depending on Ag contents. With increasing Ag content, the hole concentration increases monotonously until $x = 0.008$. More Ag introduction would not result in the apparent variety in the amount of hole, probably due to the substitution limit of Ag in $BaZn_2Sb_2$. The dependence of Ag content on hole concentration evidences the successful substitution of Ag at Zn site. Interestingly,

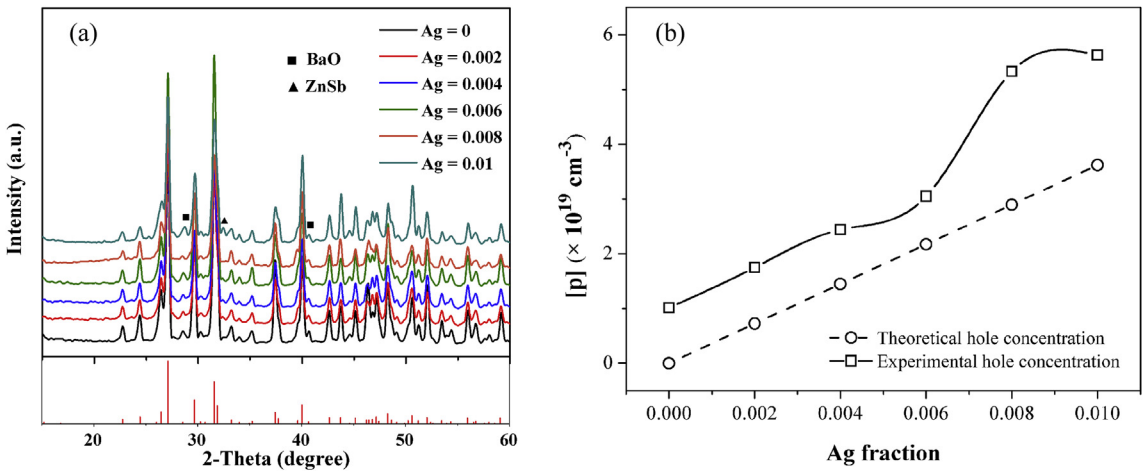

Fig. 1. PXRD patterns for the samples $Ba(Zn_{1-x}Ag_x)_2Sb_2$ and simulated patterns for reported $BaZn_2Sb_2$ (PDF#33-0095) (a), and Holes carriers concentration as function of Ag concentration in $Ba(Zn_{1-x}Ag_x)_2Sb_2$(b).